PERGAMON

Chemical Engineering Science 54 (1999) 2237–2246

Chemical Engineering Science

Gas holdup and mass transfer in bubble column reactors operated at elevated pressure

H.M. Letzel[a,b,*], J.C. Schouten[a,1], R. Krishna[b], C.M. van den Bleek[a]

[a]*Faculty of Applied Sciences, Delft University of Technology, Julianalaan 136, 2628 BL Delft, Netherlands*
[b]*Department of Chemical Engineering, University of Amsterdam, Nieuwe Achtergracht 166, 1018 WV Amsterdam, Netherlands*

Abstract

Measurements of the total gas holdup, ε, have been made in a 0.15 m diameter bubble column operated at pressures ranging from 0.1 up to 1.3 MPa. The influence of the increasing system pressure is twofold: (1) a shift of the flow regime transition point to higher gas fractions, and (2) a decrease of the rise velocity of "large" bubbles in the heterogeneous regime. The large bubble rise velocity is seen to decrease with the square root of the gas density, $\sqrt{\rho_G}$. This square root dependence can be rationalized by means of a Kelvin–Helmholtz stability analysis. The total gas holdup model of Krishna and Ellenberger (1996, A.I.Ch.E. J. 42, 2627–2634), when modified to incorporate the $\sqrt{\rho_G}$ correction for the large bubble rise velocity, is found to be in good agreement with the experimental results. The influence of system pressure on the volumetric mass transfer coefficient, k_La, is determined using the dynamic pressure-step method of Linek et al. (1993, Chem. Engng Sci. 48, 1593–1599). This pressure step method was adapted for application at higher system pressures. The ratio (k_La/ε) is found to be practically independent of superficial gas velocity and system pressure up to 1.0 MPa; the value of this ratio is approximately equal to one half. This result provides a simple method for predicting k_La using the model developed for estimation of ε.

Keywords: Bubble column; Pressure; Gas density; Holdup; Mass transfer

1. Introduction

Bubble column reactors find widespread use in industry and often these reactors are operated at elevated pressures. For example in the Fischer–Tropsch synthesis of hydrocarbons from synthesis gas (Krishna et al., 1996), the bubble column slurry reactor is operated in the pressure range of 3–4 MPa. The influence of elevated pressure on the hydrodynamics and mass transfer therefore requires careful study and analysis for design purposes.

The early cold-flow studies of Kölbel et al. (1961) suggested that there was no influence of pressure on the system hydrodynamics. This finding can be rationalized when we consider that Kölbel et al. studied only the homogeneous regime of operation. More recent studies of Clark (1990), Krishna et al. (1991), Reilly et al. (1994), Tarmy et al. (1984) and Wilkinson et al. (1992), on the other hand, showed that increasing system pressure has a significant effect on hydrodynamics. The major effect of pressure was established to be a shift of the transition from the homogeneous to the heterogeneous regime to higher gas velocities and gas holdups. Wilkinson (1991) has suggested that elevated system pressure could also have a destabilizing influence on 'large' bubbles, i.e. the bubbles ranging in size from say 15 to 50 mm, and therefore enhancing the break-up process.

The objectives of our work are (1) to further develop and quantify the idea of Wilkinson (1991) that increased pressure leads to increased break-up of 'large' bubbles, (2) to develop an estimation procedure for the total gas holdup which can be used for design purposes, and (3) to investigate the influence of increased system pressure on the volumetric mass transfer coefficient.

*Corresponding author: Present address: Shell Research and Technology Centre, Amsterdam, P.O. Box 38000, 1030 BN Amsterdam, Netherlands. Fax: 31 20 630 3079; e-mail: martijn.h.m.letzel@opc.shell.com.

[1]Present address: Eindhoven Univeristy of Technology, Laboratory of Chemical Reactor Engineering, P.O. Box 513, 5600 MB Eindhoven, Netherlands.

0009-2509/99/$ – see front matter
PII: S0009-2509(98)00418-7

2. Influence of elevated system pressure on gas holdup

2.1. Experimental

The experimental setup that was used to measure gas holdup and mass transfer is shown in Fig. 1. A glass bubble column, 0.15 m in diameter and 1.22 m high, was located in a steel pressure vessel. The liquid phase was demineralized water. Nitrogen was sparged into the column through a 0.1 m diameter perforated plate. The nitrogen supply was sufficient to obtain superficial gas velocities well into the heterogeneous regime, even at system pressures up to 1.3 MPa. The distributor was made up of 200 evenly distributed orifices, 0.5 mm in diameter, ensuring an equal initial distribution of the gas phase. The pressure in the vessel was regulated with a back pressure reducer.

In the vessel, windows of quartz–glass were located. The space between the column and the windows was also filled with demineralized water, so that visual observation without light refraction was possible. Gas holdup was measured by means of an overflow vessel, or by means of a Validyne DP 15 pressure sensor. Both methods showed a good agreement with each other.

Gas holdup measurements were done at varying gas velocities at 13 different system pressures: 0.1, 0.2, …, 1.3 MPa. A sub-set of these gas holdup data is shown in Fig. 2. A strong influence of system pressure can be observed. In order to develop a model to describe this effect we consider, in turn (1) the influence on the regime transition point, and (2) the influence on the large-bubble holdup.

2.2. Influence of gas density on the regime transition point

Both Reilly et al. (1994) and Wilkinson et al. (1991, 1992) have developed correlations for the influence of pressure on the regime transition point, in terms of influence of the gas density. In Fig. 3A and B, these correlations are compared with regime transition points, determined from gas holdups. The Reilly et al. (1994) correlation is seen to be better than the Wilkinson et al. (1991,1992) correlation. However, the Reilly correlation

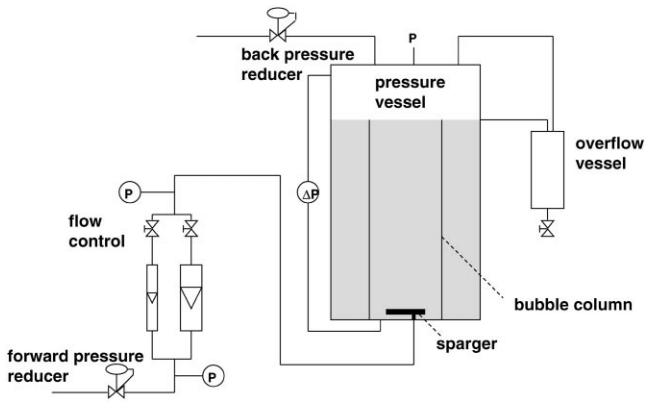

Fig. 1. Experimental setup for gas holdup measurements (nitrogen–water, column diameter 0.15 m, column height 1.22 m, system pressure ranging from 0.1 to 1.3 MPa).

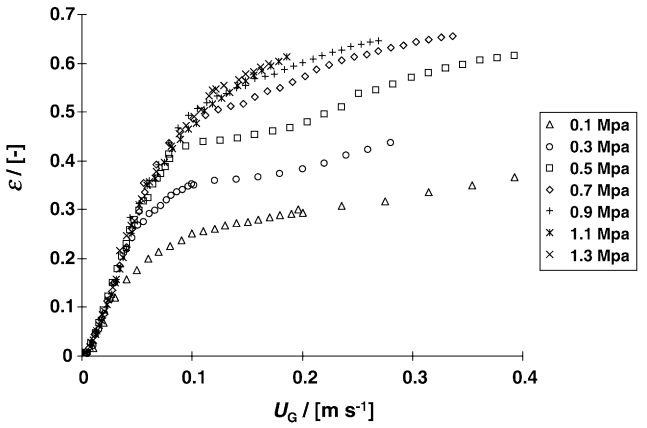

Fig. 2. Total gas holdup for nitrogen–water system as a function of superficial gas velocity at different system pressures.

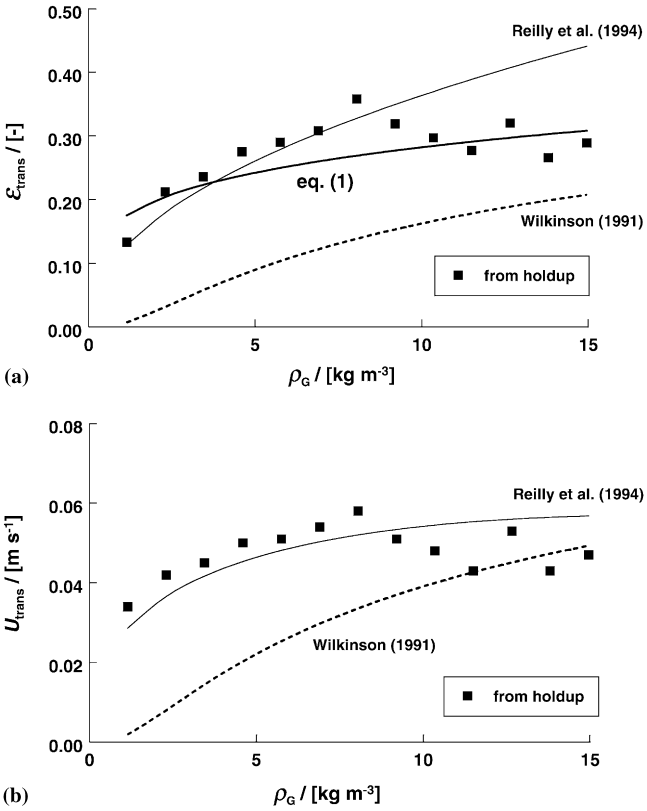

Fig. 3. Regime transition points as a function of gas density from Letzel et al. (1997) compared with correlations from Reilly et al. (1994) and Wilkinson et al. (1992): (A) total gas holdup at regime transition; (B) superficial gas velocity at regime transition.

underestimates ε_{trans} at low system pressures, and overestimates ε_{trans} at high system pressures. We see that the power-law relation

$$\varepsilon_{trans} = 0.17\rho_G^{0.22} \tag{1}$$

provides a better fit of our data.

The Reilly correlation predicts an increase of U_{trans} with ρ_g, whereas no specific trend can be found experimentally and

$$U_{trans} = 0.045\ \mathrm{m\,s^{-1}} \tag{2}$$

is an adequate description for the nitrogen–water system; see Fig. 3B.

The value of U_{trans} and ε_{trans} at different system pressures was determined before by means of chaos analysis of pressure fluctuation signals, measured in the gas–liquid dispersion (Letzel et al., 1997a). By means of the chaos analysis method, it was first observed that the value of U_{trans} stays nearly constant with increasing system pressure, whereas ε_{trans} increases. The stability theory of Batchelor (1988) and Lammers and Biesheuvel (1996) has been used to rationalize the observed shift in the transition point (Letzel et al., 1997a).

2.3. Influence of gas density on large-bubble holdup

Elevated system pressure influences the velocity of large bubbles. This can be observed from Fig. 2: at higher system pressure, the increase of gas holdup with superficial gas velocity is steeper, indicating a lower rise velocity of the large bubbles. An explanation of the lower rise velocity can be a decrease of bubble size with increasing pressure. This decrease of bubble size can be understood physically by examining the influence of system pressure on the stability of large bubbles. Use is made of the Kelvin–Helmholtz theory, as described by Lamb (1959), to describe the stability of the gas–liquid interface for infinitesimal disturbances. If the surface is unstable for a disturbance, the disturbance can grow and eventually lead to break up of the bubble. It was found that the interface is unstable for a disturbance with wave number k and velocity c, if $k^2c^2 < 0$, where

$$k^2c^2 = gk\frac{\rho_G - \rho_L}{\rho_G + \rho_L} + \frac{k^3\sigma}{\rho_G + \rho_L} - k^2\frac{\rho_G\rho_L}{(\rho_G + \rho_L)^2} \times (v_G - v_L)^2 \approx gk + \frac{k^3\sigma}{\rho_L} - k^2\frac{\rho_G}{\rho_L}v_r^2, \tag{3}$$

where ρ_G and ρ_L are the gas and liquid densities, σ is the surface tension, and $v_r = v_G - v_L$ is the relative velocity between the gas and liquid phases. We assumed that this velocity is close to the bubble rise velocity. The approximation is valid for $\rho_G \ll \rho_L$. If $k^2c^2 < 0$, a disturbance on the gas–liquid interface of a bubble grows with $\exp(\sqrt{-k^2c^2}t)$. The influence of gas density on the growth factors, apparent from Eq. (3), can therefore explain the decreased stability of the large bubbles with increased pressure, as was already suggested by Wilkinson (1991).

We have found that increasing gas density especially increases the growth factors at wave lengths in the range of 0.01 to 0.05 m. This is of the order of the size of the large bubbles (De Swart et al., 1996). Unstable disturbances can therefore occur on the gas–liquid interface of these bubbles. Therefore, large bubbles are always unstable. Nevertheless, they will still be present in the gas–liquid dispersion due to the fact that, besides a continuous process of bubble break up, there is also continuous bubble coalescence (De Swart et al., 1996). The result is a dynamic equilibrium with a corresponding equilibrium size of the large bubbles.

When gas density increases, the growth factors of unstable disturbances will increase. This will favor breakup over coalescence, shifting the equilibrium to a smaller bubble size. Together with the decreasing bubble size, the rise velocity of the bubbles also decreases. From Eq. (3) one can observe that this will decrease the growth factors and increase stability. This process goes on until a new dynamic equilibrium is reached at a smaller equilibrium bubble size.

One can conclude from Eq. (3) that two bubbles with different gas densities have the same spectrum of growth factors, if

$$\rho_G V_B^2 = \text{constant}. \tag{4}$$

Therefore, we predict from the Kelvin–Helmholtz theory that

$$V_B \propto \frac{1}{\sqrt{\rho_G}}. \tag{5}$$

To confirm this prediction, bubble velocities were estimated from gas holdups. Assuming that the increase in gas holdup in the heterogeneous regime is caused exclusively by the large bubbles, we can find the relative change of the large-bubble velocities at elevated system pressures by comparing the slope of the gas holdup in the heterogeneous regime at elevated pressure with the slope at atmospheric conditions. The results are shown in Fig. 4. The curve drawn in the figure represents the relation

$$\frac{V_B}{V_{B,atm}} = \frac{\sqrt{\rho_{atm}}}{\sqrt{\rho_G}}. \tag{6}$$

Fig. 4 shows that the experimentally observed large-bubble velocities agree well with the theoretical curve, Eq. (6). This provides strong evidence that the Kelvin–Helmholtz stability theory indeed explains the effect of system pressure on the large bubbles.

Besides providing a physical explanation for the pressure effect, the result given by Eq. (6) can also be used to adapt existing holdup correlations for large-bubble holdup, that so far have ignored the pressure effect because

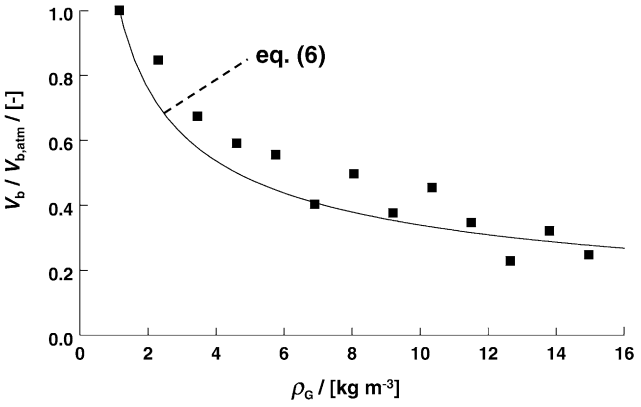

Fig. 4. Ratio of large-bubble velocities at elevated pressure and at atmospheric pressure, as a function of gas density, compared with the theoretical relation by Eq. (6).

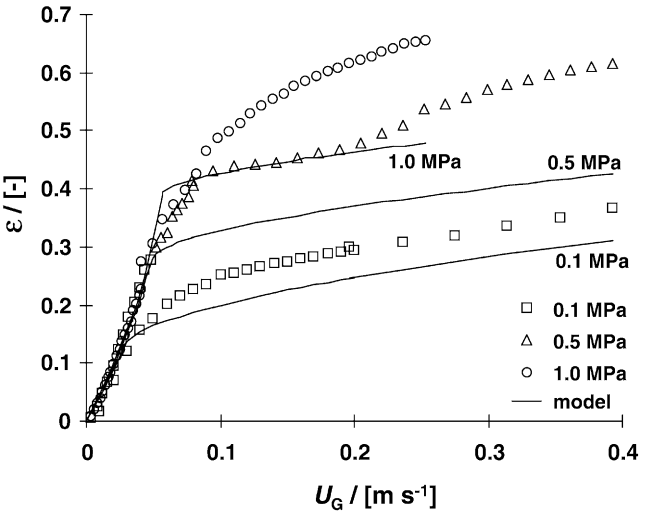

Fig. 5. Total gas holdup as a function of superficial gas velocity, calculated from Eqs. (7)–(11), compared with experimental data.

they were based on atmospheric data or data at only slightly increased gas densities.

2.4. Gas holdup model

As a basis we take the gas holdup model from Krishna and Ellenberger (1996). In the homogeneous regime, the gas holdup is described by the Richardson and Zaki (1954) relationship:

$$U = V_{\text{small}}\varepsilon(1-\varepsilon), \tag{7}$$

where V_{small} is the unhindered rise velocity of small bubbles, described by Reilly et al. (1994) as

$$V_{\text{small}} = \frac{1}{2.84}\frac{1}{\rho_G^{0.04}}\sigma^{0.12}. \tag{8}$$

For the regime transition point, Krishna and Ellenberger (1996) used the correlations of Reilly et al. (1994):

$$\varepsilon_{\text{trans}} = 0.59B^{1.5}\sqrt{\frac{\rho_G^{0.96}}{\rho_L}\sigma^{0.12}}, \tag{9}$$

$$U_{\text{trans}} = V_{\text{small}}\varepsilon_{\text{trans}}(1-\varepsilon_{\text{trans}}).$$

The large-bubble holdup is correlated by Krishna and Ellenberger (1996) as

$$\varepsilon_B = 0.268\frac{1}{D_T^{0.18}}\frac{1}{(U-U_{df})^{0.22}}(U-U_{df})^{4/5}. \tag{10}$$

The total gas holdup in the heterogeneous regime is then calculated from

$$\varepsilon = \varepsilon_B + (1-\varepsilon_B)\varepsilon_{df}, \tag{11}$$

where ε_{df} is the 'dense phase holdup', i.e. the small-bubble gas holdup, assumed to be equal to $\varepsilon_{\text{trans}}$.

Fig. 5. compares the total gas holdup, calculated from Eqs. (7)–(11) with the experimental data for a selection of our data. At atmospheric pressure, the Reilly et al. (1994) underestimates that dense phase bubble holdup. The change of large-bubble holdup with gas velocity in the heterogeneous regime is described well. At elevated pressures, however, the holdup in the heterogeneous regime is underpredicted. The Reilly et al. (1994) correlation underestimates ε_{df} at low system pressures (as noticed before) and it overestimates ε_{df} at high system pressures.

We adapt the model by using Eqs. (1) and (2) to describe the position of the regime transition point. Furthermore, the correlation given by Eq. (10) is corrected for the influence of pressure on the large-bubble rise velocity, yielding:

$$\varepsilon_B = 0.268\frac{1}{D_T^{0.18}}\frac{1}{(U-U_{df})^{0.22}}(U-U_{df})^{4/5}\left(\frac{\rho_G}{\rho_{\text{atm}}}\right)^{0.5}. \tag{12}$$

Fig. 6 compares total gas holdup, calculated from Eqs. (1), (2), (7), (8), (11) and (12) with experimental data. A good agreement is obtained. For estimation of the gas holdup in systems other than air–water, we recommend the use of Eqs. (7)–(9), (11), and (12). Fig. 7, compares these equations for the system air-water with our experimental data. Fig. 8. compares our model predictions from Eqs. (7)–(9), (11), and (12) with the experimental air–water data at different system pressures from Reilly et al. (1994). The agreement is reasonably good.

3. Influence of elevated system pressure on mass transfer

3.1. Experimental setup

A schematic of the setup for mass transfer measurements is shown in Fig. 9. The bubble column is the same

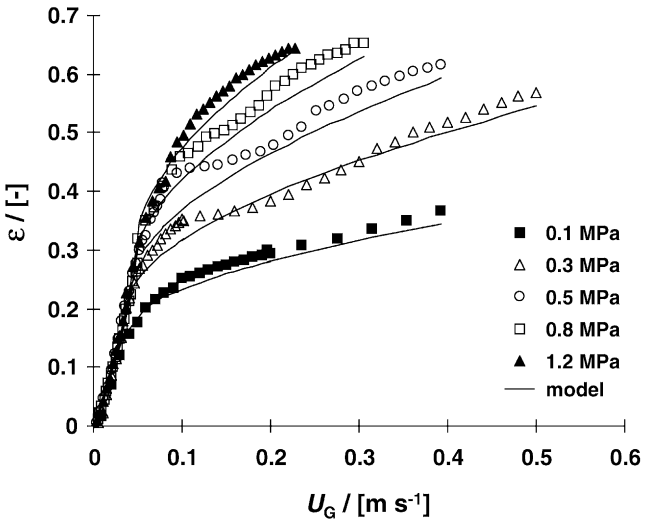

Fig. 6. Total gas holdup as a function of superficial gas velocity, calculated with Eqs. (1), (2), (7), (8), (11) and (12), compared with experimental data.

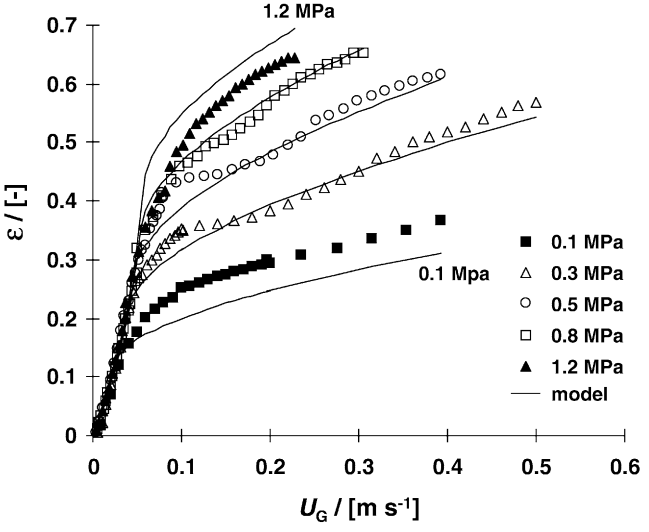

Fig. 7. Total gas holdup as a function of superficial gas velocity, calculated with Eqs. (7)–(9), (11) and (12), compared with experimental data.

as used for the gas holdup measurements. To measure the dissolved oxygen concentration in the water, a microprocessor one channel analyzer for oxygen measurement from Orbisphere Laboratories was used. The membrane of this electrode is packed in a steel housing, therefore, the electrode can be operated at elevated system pressure.

Water flows from the column through a sample tube into the sensor housing. Here it makes contact with the sensor membrane. A minimum flow of 2 ml s^{-1} is needed since oxygen diffuses through the membrane during oxygen concentration measurement. After this, the water leaves the sensor through an outlet valve. The oxygen sensor is at system pressure; the pressure drop to atmospheric pressure is over the outlet valve. With this configuration it is possible to measure oxygen concentrations at elevated system pressures. The inlet of the sample pipe is widened so that the liquid velocity is well below 0.2 m s^{-1}, making sure that no gas bubbles are present in the liquid that is sampled. Nitrogen and pressurized air can be sparged into the column.

3.2. Method

To ensure that the gas phase concentrations are known with certainty, two methods for dynamic oxygen desorption are considered: (1) the saturation method with a discontinuous switch from nitrogen to oxygen, and (2) the pressure-step method (Linek et al., 1989, 1993).

When using the first method, the water is stripped by nitrogen until the dissolved-oxygen concentration is almost nil. Then the nitrogen flow is shut down, so that all bubbles escape from the water. Then pressurized air is sparged into the column, while simultaneously the dissolved-oxygen concentration in the water is monitored. If the liquid is perfectly mixed and the oxygen depletion from the gas bubble is negligible, the dissolved-oxygen concentration is described by the relation

$$\frac{dC}{dt} = k_L a(C^* - C), \tag{13}$$

where $k_L a$ is the volumetric mass transfer coefficient, C the dissolved-oxygen concentration in the liquid bulk, and C^* the oxygen saturation concentration at the gas–liquid interface. Eq. (13) can be integrated with the boundary condition that at time t_0 (the starting point of the experiment), the dissolved oxygen concentration in the liquid bulk is zero. This yields:

$$C(t) = C^*[1 - e^{-k_L a(t-t_0)}]. \tag{14}$$

The only unknown constant in Eq. (14) is $k_L a$, which can be determined by a regression of Eq. (14) to the actual concentration data $C(t)$.

When using the second method, the pressure-step method, the vessel is simply operated at the system pressure and the gas velocity at which the $k_L a$ measurement is desired. No gas switch is needed: pressurized air is used during the entire measurement. After the operating conditions are stable, the pressure in the vessel is elevated 5–10% by pinching of the gas-outlet valve. Due to the higher pressure, the saturation concentration will increase. After saturation, the oulet valve is opened, causing the system pressure to decrease almost instantaneously to the original operating pressure. The dissolved oxygen concentration in the liquid bulk is again described by Eq. (13), however with different boundary

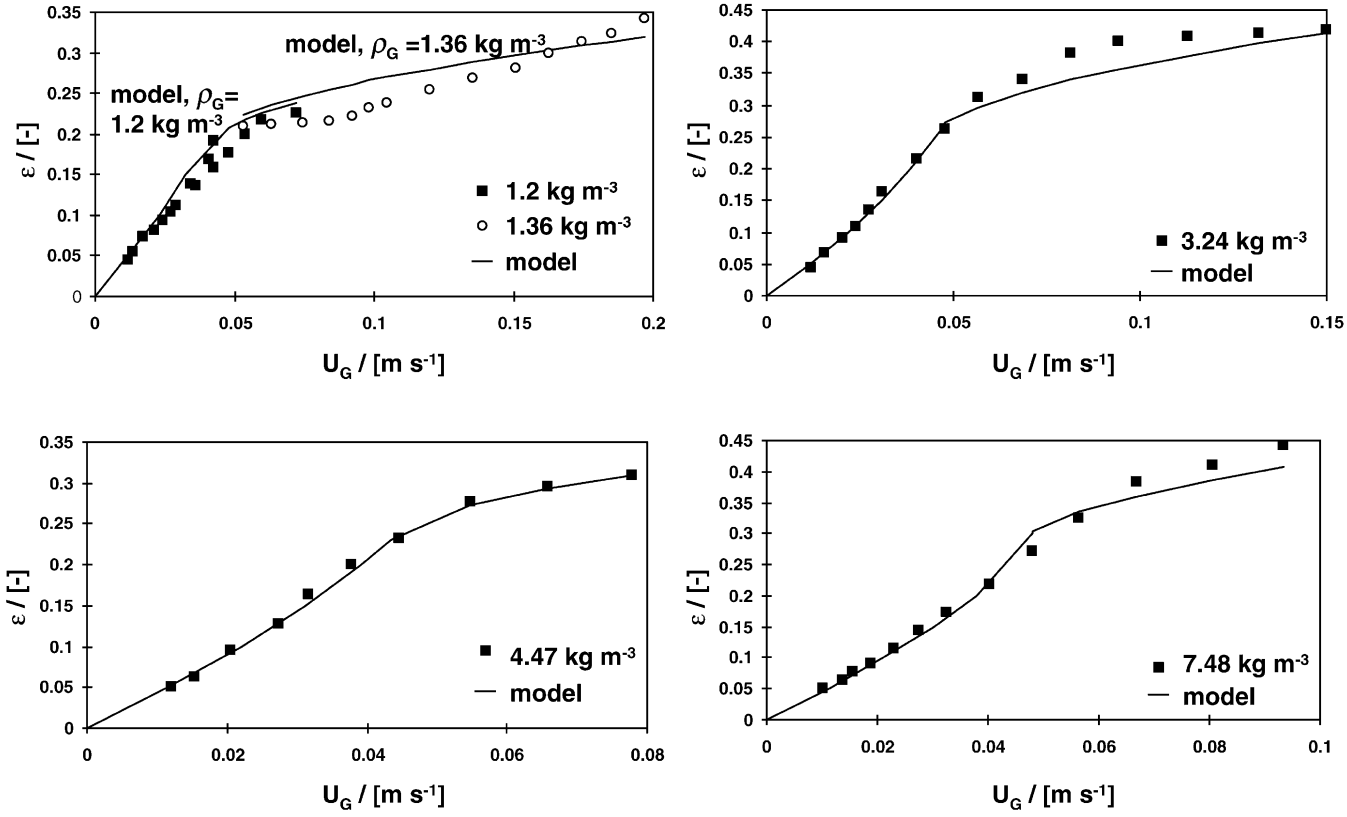

Fig. 8. Total gas holdup as a function of superficial gas velocity, calculated with Eqs. (7)–(9), (11) and (12), compared with experimental air–water data from Reilly et al. (1994) at different gas densities.

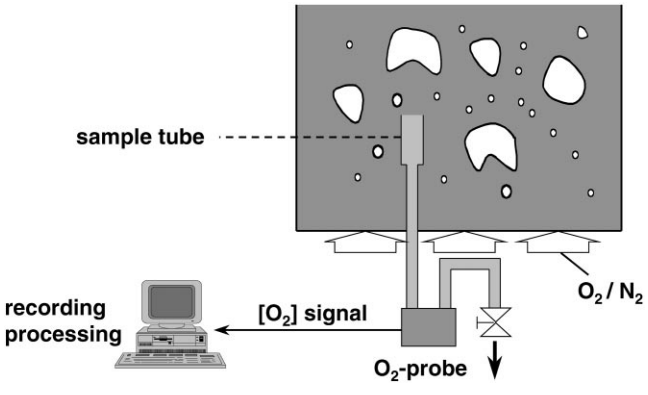

Fig. 9. Experimental setup for mass transfer measurements (nitrogen–water and air–water, column diameter 0.15 m, column height 1.22 m, system pressure ranging from 0.1 to 1.0 MPa).

conditions: at time t_0 the concentration in the liquid is C_0, the saturation concentration at the 5–10% elevated pressure. Integration of Eq. (13) now yields:

$$C(t) = C_0 e^{-k_L a(t-t_0)} + C^*[1 - e^{-k_L a(t-t_0)}]. \quad (15)$$

Again, $k_L a$ can be determined by a regression of Eq. (15) to the actual concentration $C(t)$.

3.3. Sensor response time

One can not directly use the oxygen sensor output as representing $C(t)$ in Eqs. (14) and (15), because the sensor has a finite response time. The concentration indicated by a sensor of this type, $C_{sensor}(t)$, is related to the concentration in the liquid, $C(t)$, as

$$\frac{dC_{sensor}(t)}{dt} = k_{sensor}(C(t) - C_{sensor}(t)), \quad (16)$$

where k_{sensor} is a sensor constant, quantifying the response time of the oxygen sensor. Eqs. (13) and (16) can be solved simultaneously to yield for the sensor response in case of saturation:

$$C_{sensor}(t) = C^*\left(1 - \frac{1}{k_{sensor} - k_L a}[k_{sensor} e^{-k_L a t} - k_L a e^{-k_{sensor} t}]\right), \quad (17)$$

and in the pressure-step case:

$$C_{sensor}(t) = C^* - \frac{C^* - C_0}{k_{sensor} - k_L a} \times [k_{sensor} e^{-k_L a t} - k_L a e^{-k_{sensor} t}]. \quad (18)$$

3.4. Assumptions

Several assumptions are made when using the saturation or the pressure-step method. These are:

(1) *Perfect liquid mixing*: This assumption must be fulfilled to justify for the fact that a liquid sample is taken at just one single position in the column. The mixing time of the liquid bulk must thus be much smaller than the saturation time, or:

$$\tau_{\text{mixing}} \ll \frac{1}{k_L a}. \tag{19}$$

Using data from Groen et al. (1995), Ellenberger (1995) found that the liquid circulation velocity V_{circ} can be correlated to the large-bubble velocity V_B as

$$V_B \approx \frac{4}{3} V_{\text{circ}}. \tag{20}$$

Large-bubble velocities are of the order of magnitude of $1\ \text{m s}^{-1}$. Liquid circulation velocities are thus of the same order of magnitude. Therefore, in the 0.15 m ID column used, 1.22 m high, the average liquid circulation time will be of the order of 1 s. This is well below $1/k_L a$, which is of the order of magnitude of 10 s. In case of the pressure-step method, we need only perfect mixing on the scale of adjacent gas–liquid interfaces. This condition is met far more easily than perfect mixing of the liquid bulk on the scale of the entire column. We can therefore conclude that the assumption of perfect mixing of the liquid bulk is justified.

(2) *Zero oxygen depletion*: Assuming $V_B = 0.2\ \text{m s}^{-1}$ (the velocity of small bubbles and thus the smallest bubble velocity appearing in the column), a bubble diameter of 0.004 m, and taking $k_L = 5 \times 10^{-4}\ \text{m s}^{-1}$, it can be shown that around 10% of the oxygen present in the bubble disappears during saturation. In case of a 10% pressure-step, only 1% of the oxygen disappears. In the latter case it is justified to neglect the degree of oxygen depletion, and to assume that the saturation concentration on the interface, C^*, is constant throughout the column.

(3) *Instantaneous hydrodynamic buildup*: The time needed to arrive at the steady-state hydrodynamic conditions after starting the measurement should be small compared to the saturation time. In case of the saturation method this time is unknown and might take even several minutes. With the pressure step method, the system is very close to the steady state. With a 10% pressure change, all bubbles will change 10% in volume, so they are close to their new bubble size distribution. Due to a high coalescence and breakup frequency (De Swart et al., 1996), it can be expected that this new equilibrium bubble size distribution is reached very rapidly.

(4) *Gas-side resistance*: To find the effect of elevated system pressure on the liquid-side volumetric mass transfer coefficient, one must be sure that the change with changing pressure of the gas-side mass transfer coefficient, $k_G a$, does not influence the results. This condition is met when $k_G a$ is much larger than $k_L a$ at all system pressures of interest. The ratio $k_G a / k_L a$ is approximately equal to (Cho and Wakao, 1988, Wilkinson et al., 1994):

$$\frac{k_G a}{k_L a} = \frac{k_G}{k_L} \approx 10 \sqrt{\frac{D_G}{D_L}} \approx 10^3. \tag{21}$$

Eq. (21) holds at atmospheric pressure. The gas-side mass transfer coefficient k_G is, however, inversely proportional to the square root of system pressure (Oyevaar and Westerterp, 1989, Wilkinson et al., 1994). Therefore, the ratio by Assumption (2) will decline with elevated pressure. For air–water, gas-phase resistance remains negligible compared to liquid phase resistance at pressures up to 10 MPa (at 10 MPa, the gas-phase resistance is still two orders of magnitude smaller than the liquid-phase resistance). Therefore, the $k_L a$-measurements will not be influenced by a changing $k_G a$.

We can conclude that the liquid in the system can be considered to be perfectly mixed on the time scale of the $k_L a$ measurement. The conditions of zero depletion and instantaneous hydrodynamic buildup are easily met by the pressure-step method. In case of the saturation method there is doubt about the hydrodynamic buildup. Concluding, we can say that the pressure-step method is the preferred method in practice. A further practical advantage of the pressure-step method is its experimental ease.

4. Results

Fig. 10 shows an example of the output signal of the oxygen probe at a superficial gas velocity of $0.058\ \text{ms}^{-1}$, at atmospheric system pressure. The continuous curve is the fit by Eq. (18). With this fit, both $k_L a$ and k_{sensor} are determined: $k_L a = 0.099\ \text{s}^{-1}$ and $k_{\text{sensor}} = 0.505\ \text{s}^{-1}$. Fig. 11. shows values for k_{sensor} from all the experiments done in this work. The average is equal to 0.5s^{-1}. The $k_L a$ values were determined again by a data fit, using this average value of k_{sensor}.

Fig. 12 shows $k_L a$ as a function of superficial gas velocity for system pressures of 0.1, 0.2, 0.3 and 0.4 MPa, respectively. At every value for the superficial gas velocity, the $k_L a$ values were determined three times. At lower pressures, deviation from the average value was well below 10%. At 0.4 MPa, the deviation deteriorated to approximately 20%. Fig. 12. shows the average value of every triplet. A clear influence of system pressure on the value of the volumetric mass transfer coefficient can be observed.

Simultaneously with the volumetric mass transfer coefficient, the total gas holdup was determined. Fig. 13.

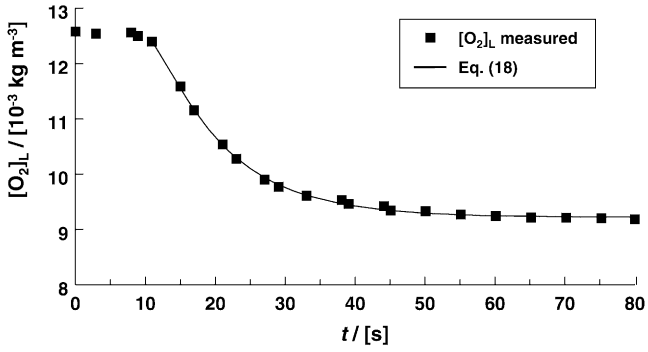

Fig. 10. Example of a mass transfer measurement using the pressure-step method, together with a least-squares fit of Eq. (18).

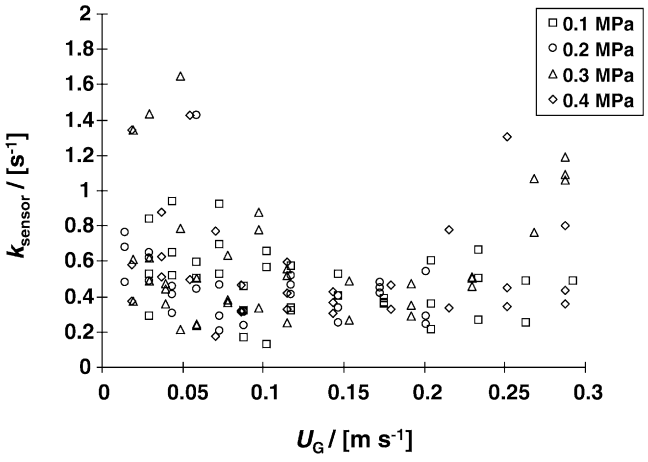

Fig. 11. Sensor constant, k_{sensor}, determined experimentally by a least-squares fit of Eq. (18) for all measurement points at different system pressures and superficial gas velocities.

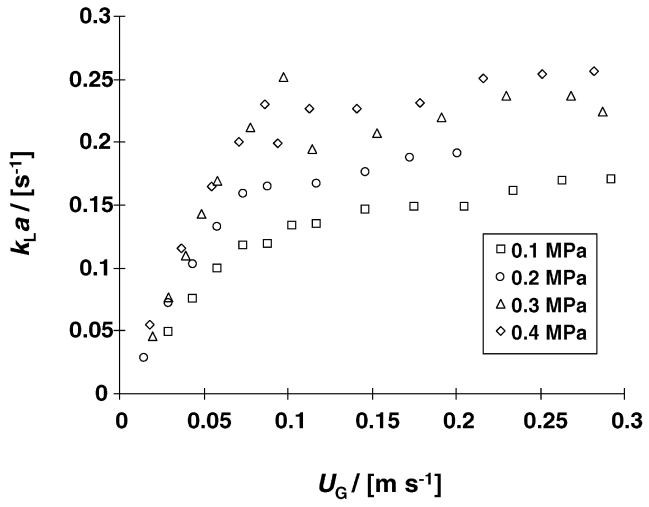

Fig. 12. Volumetric mass transfer coefficient, k_La, as a function of superficial gas velocity at different system pressures.

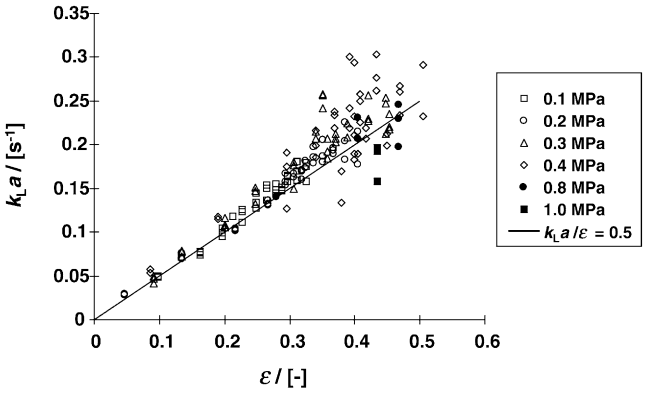

Fig. 13. Volumetric mass transfer coefficient, k_La, as a function of the total gas holdup at different system pressures.

shows the values for the volumetric mass transfer coefficient as a function of the total gas holdup. It can be observed that total gas holdup uniquely determines k_La: the ratio k_La/ε is constant and equal to approximately one half. This result confirms the similar observation by Vermeer and Krishna (1981) and it shows that an accurate prediction of the total gas holdup is sufficient to predict the volumetric mass transfer coefficient in a bubble column at elevated pressure.

Determination of k_La was not possible at pressures above 0.4 MPa when using pressurized air, because the saturation concentration of the oxygen sensor is 40×10^{-3} kg m^{-3}. This problem could be overcome by using a mixture of nitrogen/pressurized air. In this way, it was possible to keep the saturation concentration of oxygen in water below 40×10^{-3} kg m^{-3} at all system pressures. Several k_La measurements were done at system pressures of 0.8 and 1.0 MPa, respectively. The results are included in Fig. 13. One can observe that the ratio k_La/ε is constant and equal to approximately one half, up to system pressures of 1.0 MPa.

At gas holdups larger than 35%, the scatter in k_La increases. The reason is that at higher gas holdups, the value of k_La approaches that of k_{sensor}. In this case the fit of Eq. (18) becomes inaccurate for determination of k_La. The method works best when k_La is less than say one half of the value of k_{sensor}. The accuracy and the range of k_La values is therefore limited by k_{sensor}, which should be as high as possible. Sensors with high k_{sensor} however have a low oxygen saturation concentration. If pressurized air is used as gas phase, this means that the system pressure at which the probe can be used is limited. This problem can be overcome with the concept of dilution of air with nitrogen, as presented above. In this way, sensors with low saturation concentrations (but fast response) can be used at any system pressure desired.

For the estimation of the volumetric mass transfer coefficient at elevated pressure, the result $k_La/\varepsilon = 0.5$ can be used, together with the model for the total gas holdup developed in this work.

5. Conclusions

The influence of elevated system pressure on gas holdup and mass transfer in bubble columns has been studied. Experimental gas holdup data were obtained in a column operated at system pressures up to 1.3 MPa.

The influence of gas density on the regime transition point in a nitrogen–water system can be described with Eqs. (1) and (2). The correlations of Reilly et al. (1994) for the transition point are closer to these values than the correlations of Wilkinson et al. (1991, 1992). The Reilly et al. (1994) correlation however underestimates ε_{trans} at 0.1 MPa, and it overestimates ε_{trans} at the upper end of the pressure range investigated.

Based on a Kelvin–Helmholtz stability analysis of the gas–liquid interface, the rise velocity of large bubbles was predicted to be inversely proportional to the square root of the gas density. Based on this insight, the correlation for large-bubble holdup from Krishna and Ellenberger (1996) was adapted to account for this effect.

A model for total gas holdup was formulated. It was based on Krishna and Ellenberger (1996), using Eqs. (1) and (2) to describe the position of the transition point for the nitrogen–water system, and using our insights about the influence of pressure on large-bubble velocity to adapt the correlation for large-bubble holdup. A good agreement was found between the model and the total gas holdup data obtained in this work. For systems other than air–water, we recommend the correlation of Reilly et al. (1994) for the regime transition point.

Using the dynamic pressure-step method of Linek et al. (1989, 1993), the volumetric mass transfer coefficient was determined at system pressures of 0.1–1.0 MPa. The assumptions made (perfect liquid mixing, zero depletion, fast hydrodynamic buildup) were satisfied easily using this method under the conditions studied. The method was adapted for usage at high system pressures.

A strong influence of system pressure on k_La was found. The increase of k_La with increasing pressure was shown to be caused by the increase in total gas holdup: the ratio k_La/ε was shown to be constant and to have a value of approximately one half.

This insight, together with the model for holdup at elevated pressure, enables one to predict mass transfer coefficients at different system pressures in gas–liquid bubble columns.

Acknowledgements

The authors gratefully acknowledge financial support from the Dutch foundation for chemical research (SON), DSM, and AKZO NOBEL, as well as experimental facilities provided by DSM Research. The authors wish to thank Dr. A. Stankiewicz (DSM Research) for discussions and support.

Notation

a	gas–liquid interfacial area per unit liquid volume, m^{-1}
B	constant in the Reilly et al. (1994) correlation, Eq. (9), dimensionless
c	wave velocity of disturbance on gas liquid interface, $m\,s^{-1}$
C	liquid oxygen concentration, $10^{-3}\,kg\,m^{-3}$
C_0	liquid oxygen concentration at start of measurement, $10^{-3}\,kg\,m^{-3}$
C^*	oxygen saturation concentration, $10^{-3}\,kg\,m^{-3}$
C_{sensor}	oxygen concentration indicated by sensor, $10^{-3}\,kg\,m^{-3}$
d	bubble diameter, m
d_s	Sauter mean diameter of bubble, m
D_G	oxygen diffusivity in gas, m^2s^{-1}
D_L	oxygen diffusivity in liquid, m^2s^{-1}
D_T	column diameter, m
g	gravitational constant, $m\,s^{-2}$
k	wave number, m^{-1}
k_G	gas-side mass transfer coefficient, $m\,s^{-1}$
k_L	liquid-side mass transfer coefficient, $m\,s^{-1}$
k_{sensor}	sensor response constant, s^{-1}
N	stability parameter, dimensionless
t	time, s
t_0	time at start of mass transfer measurement, s
U	superficial gas velocity, $m\,s^{-1}$
U_{df}	superficial gas velocity in the dense phase, $m\,s^{-1}$
U_{ins}	superficial gas velocity at instability point, $m\,s^{-1}$
U_{swarm}	bubble swarm velocity, $m\,s^{-1}$
U_{trans}	superficial gas velocity at transition point, $m\,s^{-1}$
v_G	fluid velocity at gas-side of interface,ms^{-1}
v_L	fluid velocity at liquid-side of interface, $m\,s^{-1}$
v_r	relative velocity between gas and liquid at interface, $m\,s^{-1}$
V_B	large-bubble velocity, $m\,s^{-1}$
$V_{B,atm}$	large-bubble velocity at atmospheric pressure, $m\,s^{-1}$
V_{circ}	liquid circulation velocity, $m\,s^{-1}$
V_{small}	small-bubble velocity, $m\,s^{-1}$

Greek letters

ε	total gas holdup, dimensionless
ε_B	large-bubble gas holdup, dimensionless
ε_{df}	small-bubble gas holdup, dimensionless
ε_{ins}	gas holdup at instability point, dimensionless
ε_{trans}	gas holdup at transition, dimensionless
μ_L	liquid viscosity, Pa s
ρ_{atm}	gas density at atmospheric pressure, $kg\,m^{-3}$
ρ_G	gas density, $kg\,m^{-3}$

ρ_L	liquid density, $\mathrm{kg\,m^{-3}}$
ρ_{sys}	gas density at system pressure, $\mathrm{kg\,m^{-3}}$
σ	surface tension, $\mathrm{N\,m^{-1}}$
τ_{mixing}	mixing time of liquid phase, s

Subscripts

0	referring to time $t = 0$
atm	atmospheric conditions
df	referring to dense phase
B	referring to large bubbles
G	referring to gas phase
ins	at instability point
L	referring to liquid phase
sys	referring to system pressure
small	referring to small bubbles
swarm	referring to bubble swarm
trans	referring to regime transition point
T	referring to tower or column

References

Batchelor, G.K. (1988). A new theory of the instability of a uniform fluidized bed. *J. Fluid Mech.*, *193*, 75–110.

Cho, J.S., & Wakao, N. (1988). Determination of liquid-side gas-side volumetric mass transfer coefficients in a bubble column. *Chem. Engng Jpn*, *21*, 576–581.

Clark, K.N. (1990). The effect of high pressure and temperature on phase distributions in a bubble column. *Chem. Engng Sci.*, *45*, 2301–2307.

Ellenberger, J. (1995). *Analogies in Multiphase reactor hydrodynamics*, Ph.D. Thesis, University of Amsterdam, The Netherlands.

Groen, J.S., Mudde, R.F., & Van den Akker, H.E.A. (1995). Time dependent behavior of the flow in a bubble column. *Trans. Inst. Chem. Engrs*, *73*, 615–621.

Kölbel, H., Borchers, E., & Langemann, H. (1961). Grössenverteilung der gasblasen in blasensaulen. *Chem. Ing. Technol.*, *33*, 668–675.

Krishna, R., & Ellenberger, J. (1996). Gas holdup in bubble column reactors operating in the churn-turbulent flow regime. *A.I.Ch.E. J.*, *42*, 2627–2634.

Krishna, R., Ellenberger, J., & Sie, S.T. (1996). Reactor development for conversion of natural gas to liquid fuels: a scale-up strategy relying on hydrodynamic analogies *Chem. Engng Sci.*, *51*, 2041–2050.

Krishna, R., Wilkinson, P.M., & Van Dierendonck, L.L. (1991). A model for gas holdup in bubble columns incorporating the influence of gas density on flow regime transitions. *Chem. Engng Sci.*, *46*, 2491–2496.

Lamb, H. (1959). Hydrodynamics (6th ed.). Cambridge: Cambridge University Press.

Lammers, J.H., & Biesheuvel, A. (1996). Concentration waves and the instability of bubbly flows. *J. Fluid Mech.*, *328*, 67–93.

Letzel, H.M., Schouten, J.C., Van den Bleek, C.M., & Krishna, R. (1997a). Influence of elevated pressure on the stability of bubbly flows. *Chem. Engng Sci.*, *52*, 3733–3739.

Letzel, H.M., Schouten, J.C., Krishna, R., & Van den Bleek, C.M. (1997b). Characterization of regimes and regime transitions in bubble columns by chaos analysis of pressure signals. *Chem. Engng Sci.*, *54*, 4447–4459.

Linek, V., Benes, P., & Vacek, V. (1989). Dynamic pressure method for k_La measurement in large-scale bioreactors. *Biotechnol. Bioengng*, *33*, 1406–1412.

Linek, V., Benes, P., Sinkule, J., & Moucha, T. (1993). Non ideal pressure step method for k_La measurement. *Chem. Engng Sci.*, *48*, 1593–1599.

Oyevaar, M.H., & Westerterp, K.R. (1989). Mass transfer phenomena and hydrodynamics in agitated gas–liquid reactors and bubble columns at elevated pressures: state of the art. *Chem. Engng Process.*, *25*, 85–98.

Reilly, I.G., Scott, D.S., De Bruijn, T.J.W., & MacIntyre, D. (1994). The role of gas phase momentum in determining the gas holdup and hydrodynamic flow regimes in bubble column operations. *Can. J. Chem. Engng*, *72*, 3–12.

Richardson, J.F., & Zaki, W.N. (1954). Sedimentation and fluidisation: Part I. *Trans. Inst. Chem. Engrs*, *32*, 35.

Swart, J.W.A. de, Van Vliet, R.E., & Krishna, R. (1996). Size, structure and dynamics of 'large' bubbles in a two-dimensional slurry bubble column. *Chem. Engng Sci.*, *51*, 4619–4629.

Tarmy, B.L., Chang, M., Coulaloglou, C.A., & Ponzi, P.R. (1984). The three phase characteristics of the EDS coal liquefaction reactors: their development and use in reactor scale up. *Inst. Chem. Engng Symp. Ser.*, *87*, 303–317.

Vermeer, D.J., & Krishna, R. (1981). Hydrodynamics and mass transfer in bubble columns operating in the churn-turbulent regime. *Ind. Engng Chem. Process Des. Dev.*, *20*, 475–482.

Wilkinson, P.M. (1991). *Physical Aspects and scale-up of high pressure bubble columns*, Ph.D. thesis, University of Groningen, The Netherlands.

Wilkinson, P.M., Spek, A.P., & Van Dierendonck, L.L. (1992). Design parameters estimation for scale-up of high pressure bubble columns. *A.I.Ch.E. J.*, *38*, 544–554.

Wilkinson, P.M., Haringa, H., & Van Dierendonck, L.L. (1994). Mass transfer and bubble size in a bubble column under pressure. *Chem. Engng Sci.*, *49*, 1417–1427.